
ELECTRICAL AND MAGNETIC
PROPERTIES

Effect of Scandium Additions on the Temperature Dependences of the Heat Capacity and Thermodynamic Functions of Aluminum–Manganese Alloys

I. N. Ganiev^{a, *}, M. T. Norova^b, B. B. Eshov^b, N. F. Ibrokhimov^c, and S. Zh. Ibrokhimov^c

^a*Nikitin Institute of Chemistry, Academy of Sciences of the Republic of Tajikistan, Dushanbe, 734063 Tajikistan*

^b*State Research Institution Research Center for Innovative Technologies of the Academy of Sciences of the Republic of Tajikistan,
Dushanbe, 734063 Republic of Tajikistan*

^c*Osimi Tadjik Technical University, Dushanbe, 734042 Republic of Tajikistan*

*e-mail: ganiev48@mail.ru

Received May 6, 2019; revised June 25, 2019; accepted July 10, 2019

Abstract—The “cooling” method based on the Newton–Richmann law is used to measure specific heat capacity. It is shown that, as the manganese concentration in aluminum–magnesium alloys and temperature increase, the specific heat capacity of the alloys increases; as the scandium concentration increases, the heat capacity slightly decreases. As the temperature increases, the specific enthalpy and entropy of the alloys increase, whereas the specific Gibbs energy decreases. Scandium additions almost do not affect changes in thermodynamic functions of the alloys.

Keywords: aluminum, magnesium alloys, scandium, “cooling” mode, heat capacity, enthalpy, entropy, Gibbs energy

DOI: 10.1134/S0031918X20010068

INTRODUCTION

Aluminum–magnesium alloys are widely used in industry. A wide group of industrial alloys, such as of type AMg1, AMg2, AMg3, AMg4, and AMg6 are classified among the Al–Mg alloys. As the magnesium concentration in magnalium alloys increases, the hardness and fatigue strength increase, whereas the plasticity decreases. These alloys are characterized by high plasticity, adequate weldability, and high corrosion resistance.

To improve the properties of magnalium alloys, they are alloyed with various components. It should also be noted that the development of new compositions of Al-based alloys with the given characteristics is possible when data on the thermodynamic properties of each of the components comprising the system are available. The modification of aluminum alloys with metals, particularly rare-earth metals, which are poorly soluble or almost insoluble in solid aluminum and form various chemical compounds with aluminum, is promising [1–7].

The study of heat capacity is one of the main methods used for investigating structural and phase transformations in alloys. The temperature dependence of heat capacity allows one to determine other physical characteristics of a solid, such as the temperature and the kind of phase transformation, Debye temperature,

vacancy formation energy, electronic heat capacity coefficient, etc.

THEORY AND EXPERIMENTAL

The Newton–Richmann law of cooling is used to measure the specific heat capacity of alloys over a wide temperature range. Any body that has a temperature higher than that of the environment will cool and the cooling rate will depend on the heat capacity of the body. If we take two metallic samples with the same shape and cool them from the same temperature, the measured cooling curves allow one to determine the heat capacity of one of the samples if the heat capacity of the other sample (standard) is available.

The amount of heat that is lost by a metal volume dV for time $d\tau$ is equal to

$$\delta Q = C_p^0 \rho \frac{dT}{d\tau} dV d\tau, \quad (1)$$

where C_p^0 is the specific heat capacity of metal; ρ is the density of metal; and T is the temperature of the sample (which is taken to be the same for all points of the sample since the linear sizes of the sample are small and its thermal conductivity is high).

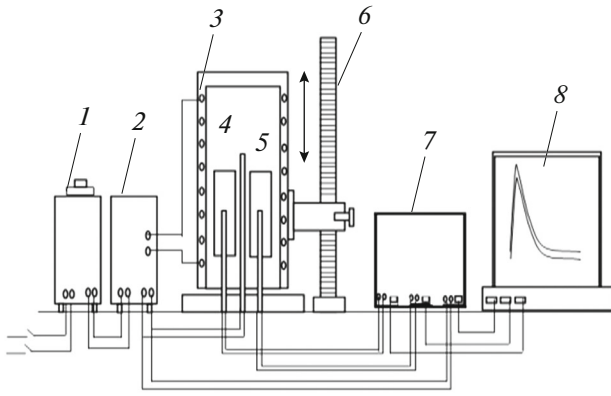


Fig. 1. Schematic diagram of installation for the determination of heat capacity of solids in regime of cooling: (1) autotransformer; (2) thermocontroller; (3) electric furnace; (4) studied sample; (5) standard; (6) electric furnace base; (7) multichannel digital thermometer; and (8) recording instrument (computer).

The value of δQ can be calculated by law:

$$\delta Q = \alpha(T - T_0)dSd\tau, \quad (2)$$

where dS is the surface area; T_0 is the ambient temperature; and α is the heat-transfer coefficient.

Equating Eqs. (1) and (2), we obtain

$$C_p^0 \rho \frac{dT}{d\tau} dV = \alpha(T - T_0)dS. \quad (3)$$

Assuming that C_p^0 , ρ , and $\frac{dT}{d\tau}$ are independent of coordinates of points of the sample volume and α , T , and T_0 are independent of coordinates of points of the sample surface, we can write

$$C_p^0 \rho V \frac{dT}{d\tau} = \alpha(T - T_0)S \quad (4)$$

or

$$C_p^0 m \frac{dT}{d\tau} = \alpha(T - T_0)S, \quad (5)$$

where V is the volume of the whole of the sample, $\rho V = m$ is the mass; and S is the whole surface area of the sample. In assuming that $S_1 = S_2$, $T_1 = T_2$, and $\alpha_1 = \alpha_2$, Eq. (5) for two samples of the same size can be represented as:

$$C_{p_2}^0 = C_{p_1}^0 \frac{m_1}{m_2} \frac{\left(\frac{dT}{d\tau}\right)_1}{\left(\frac{dT}{d\tau}\right)_2} = C_{p_1}^0 \frac{m_1}{m_2} \frac{\left(\frac{\Delta T}{\Delta \tau}\right)_1}{\left(\frac{\Delta T}{\Delta \tau}\right)_2}, \quad (6)$$

where $m_1 = \rho_1 V_1$ is the mass of the first sample; $m_2 = \rho_2 V_2$ is the mass of the second sample; and $\left(\frac{dT}{d\tau}\right)_1$, $\left(\frac{dT}{d\tau}\right)_2$ are the cooling rates of standard and studied sample at a given temperature.

Therefore, if the masses of samples m_1 and m_2 , the cooling rates of standard and studied sample, and specific heat capacity of standard $C_{p_1}^0$ are available, the specific heat capacity $C_{p_2}^0$ of the studied sample can be calculated using the right side of Eq. (6).

The heat capacity was measured using an installation, schematic diagram of which is shown in Fig. 1. Electric furnace 3 is mounted on a bench and can be moved on it to the right or to the left. Sample 4 (can also be moved) is a cylinder 30 mm in height and 16 mm in diameter and has a channel drilled at one end, in which a thermocouple is inserted. Ends of the thermocouple were attached to a Digital Multimeter UT71B 7 measuring device, which directly records results of measurements in tabulated form with computer 8. The tabulated data were used to plot cooling curves for samples of studied alloys.

RESULTS AND DISCUSSION

The aluminum–manganese alloys were synthesized under a flux using a SShOL laboratory shaft furnace and A7 grade aluminum (State standard GOST 11069–2001), Mg95 grade manganese (State standard GOST 804–93), and an Al-based master alloy containing 2.0 wt % Sc. The manganese contents in the AMg2, AMg3, and ANg4 alloys were 2, 3, and 4 wt %, respectively. Magnesium was wrapped in an aluminum foil and made a part of aluminum-based melt. The scandium content in the alloys was 0.01, 0.05, 0.1, and 0.5 wt %, respectively.

The composition of the alloy was determined by atomic emission spectroscopy using a DFS-452 diffraction spectrograph equipped with an MORS-9 multichannel optical recording system. An electric arc was used as the excitation source. Figure 2 shows analytical lines, which correspond to magnesium and scandium and indicate the presence of the elements and impurities in the alloys.

Study of the Microstructure of Alloys

Microsections of studied alloys were prepared by grinding, polishing, and etching and were used for metallographic analysis. Samples were cut using a hand saw while preventing substantial heating of samples. The microsection sizes were 1.5–2.0 cm². The samples were subjected to etching in a 20% NaOH aqueous solution upon heating to 60–70°C. After etching, a microsection was rinsed with water and carefully dried. The structure of alloys was studied with a magnification of $\times 200$ using a NEOPHOT-31 optical microscope.

As an example, Fig. 3 shows the microstructure of the AMg4 alloy with scandium. Our studies allowed us to find that the structure of alloys is of the same type and consists of the aluminum solid solution. Particles

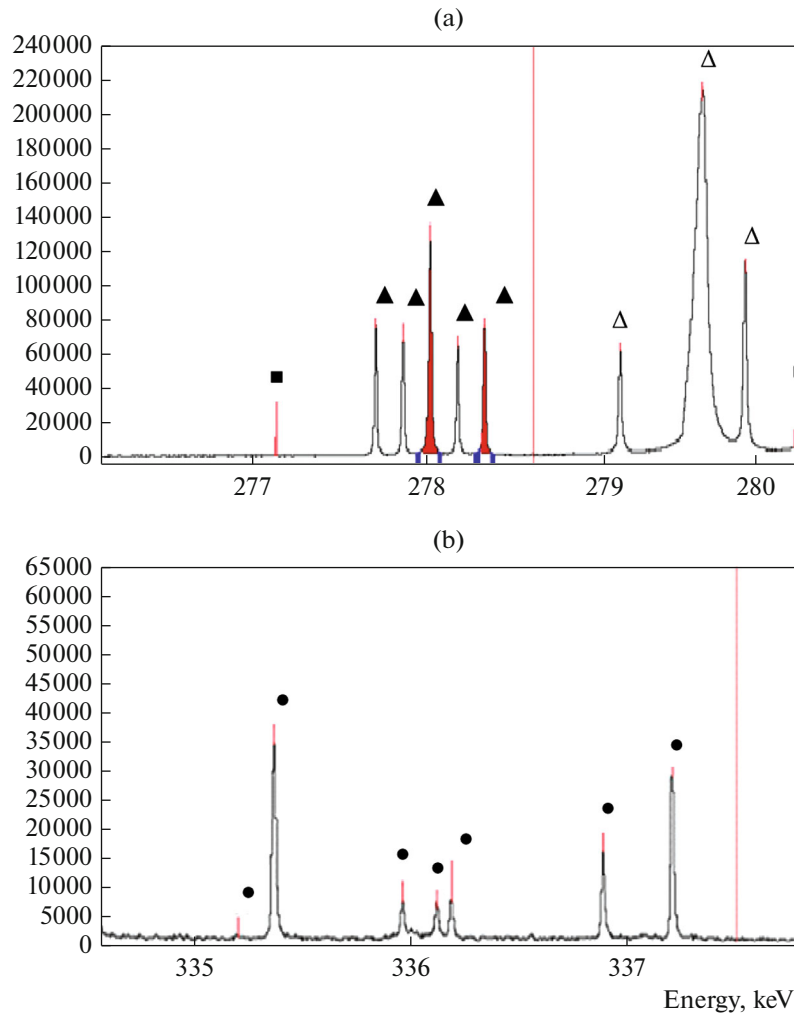


Fig. 2. Atomic emission spectra of (a) magnesium and zinc and (b) scandium in the AMg4 alloy: (▲) Mg, (△) Mg⁻, (■) Zn, (●) Sc.

of intermetallic phases (particularly Mg₂Al₃) formed in the course of alloy solidification are also observed. The amount and sizes of the second phase ultimately affect the different properties of the initial alloy. It is seen that scandium additions in the AMg4 alloy refine the structure and it becomes uniform and fine-grained.

Study of the Specific Heat Capacity of Alloys

The temperature dependence of the heat capacity and changes in the thermodynamic properties of the AMg2, AMg3, and AMg4 alloys with scandium were measured in accordance with methods described in [8–15].

The heat capacity of the AMg2, AMg3, and AMg4 alloys with scandium was measured in a cooling regime. The temperature was measured using a multi-channel digital thermometer, which allows one to directly record results of measurements in tabular form on a computer. The accuracy of measurements of

the temperature was 2°C. The time interval of temperature recording was 10 seconds. The relative error of the temperature measurement in a temperature range of 40 to 800°C was ±1.5%. The error of heat capacity measurements in accordance with the used method does not exceed 1.5% (Tables 1 and 2).

Table 1. Experimental cooling rates ($dT/d\tau$, K/s) of M00 grade copper samples

T , K	Measurement no.		
	1	2	3
300	0.0	0.0	0.0
400	0.2	0.1	0.1
500	0.4	0.2	0.2
600	0.5	0.3	0.3
700	0.7	0.6	0.4
800	0.8	0.8	0.4

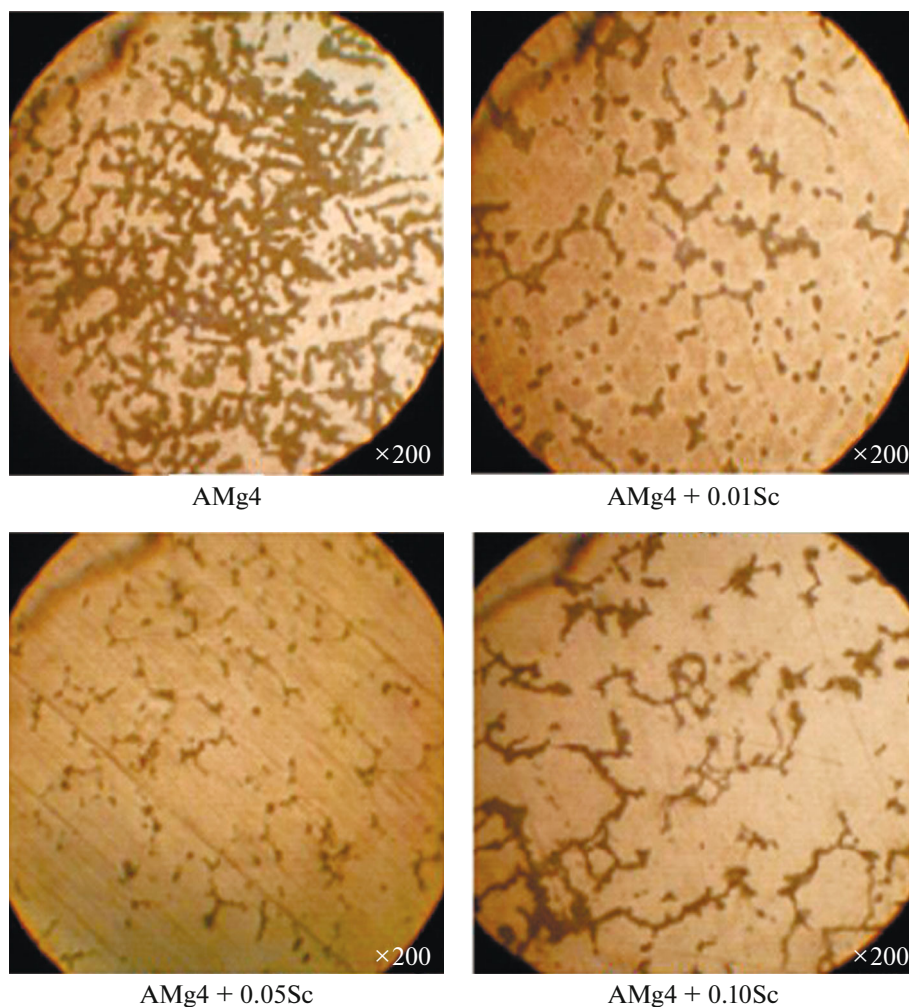


Fig. 3. Microstructure of the AMg4 alloy with different scandium contents.

Results of the measurements were processed using MS Excel software. The dependences were plotted using Sigma Plot software. The correlation coefficient was $R_{\text{corr}} > 0.9544$; it confirms the accuracy of the used approximating function.

To determine the error of the method, the heat capacity of M00 grade copper was previously measured with respect to A7 grade aluminum. Tables 1 and 2 show the results of three parallel measurements. As is seen, the found errors of the measurements of the

Table 2. Specific heat capacity (kJ/kg K) of M00 grade copper

T, K	Heat capacity of M00 grade copper [16]	Heat capacity of M00 grade copper determined experimentally with respect to A7 grade aluminum		
		measurement no.		
		1	2	3
300	0.3850	0.3759	0.3699	0.3678
400	0.3977	0.3883	0.3820	0.3800
500	0.4080	0.3984	0.3919	0.3899
600	0.4169	0.4070	0.4004	0.3984
700	0.4251	0.4151	0.4083	0.4064
800	0.4336	0.4234	0.4164	0.4146

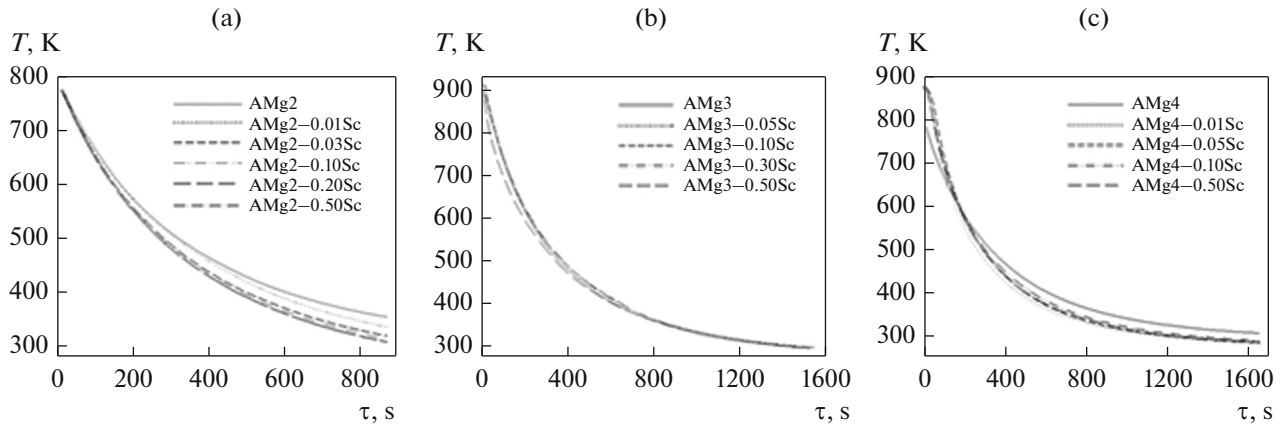


Fig. 4. Dependences of the temperature of samples (T) on the cooling time (τ) for the (a) AMg2, (b) AMg3, and (c) AMg4 alloys with scandium.

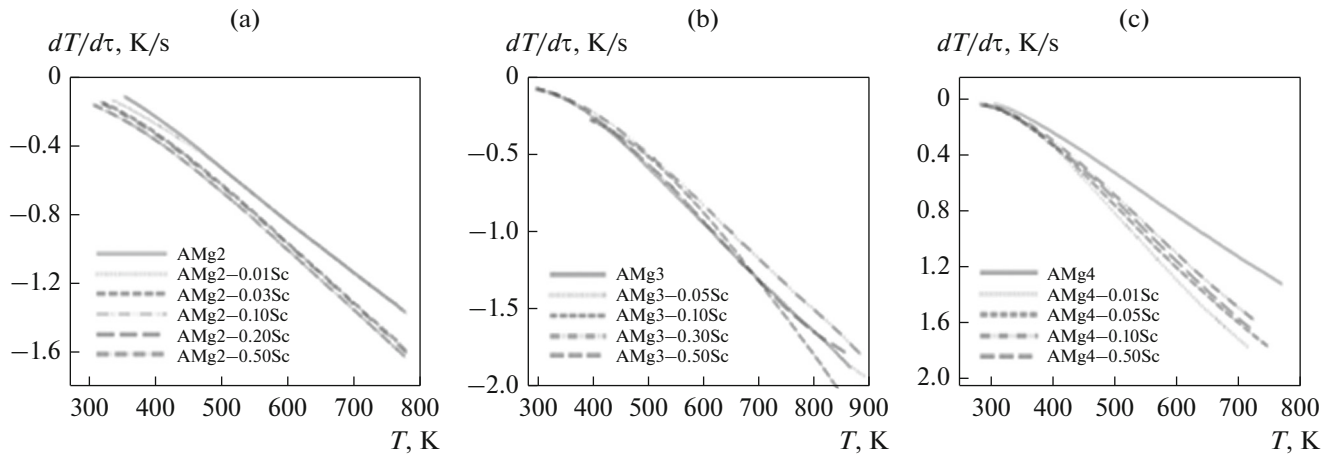


Fig. 5. Temperature dependences of the cooling rate of samples of the (a) AMg2, (b) AMg3, and (c) AMg4 alloys with scandium.

heat capacity of M00 grade copper do not exceed 1.5%. Further in the present study, we used M00 copper as the standard, which is a reliable metal since it has a higher melting temperature and is characterized by reliable values of heat capacity determined by many investigators using different methods [15, 16].

The comparison of experimentally obtained values of the heat capacity of copper with the tabulated data [16] indicates their 99% convergence.

Figure 4 shows the measured cooling curves for the AMg2, AMg3, and AMg4 alloys with scandium. The obtained temperature dependences of the alloys (Fig. 4) are described by expression

$$T = a \exp(-b\tau) + p \exp(-k\tau), \quad (7)$$

where a , b , p , and k are constants for the sample and τ is the cooling time.

The differentiation of Eq. (7) with respect to τ allows us to obtain the equation for the determination of the cooling rate of alloys

$$\frac{dT}{d\tau} = -abe^{-b\tau} - pke^{-k\tau}. \quad (8)$$

The values of coefficients a , b , p , k , ab , and pk in Eq. (8) were calculated.

Figure 5 shows curves of the cooling rate of alloys with a regression coefficient of no less than 0.998.

The calculated cooling rates of samples were used to calculate the specific heat capacity of the alloys by Eq. (6). The polynomials describing the temperature dependence of the specific heat capacity of the AMg2, AMg3, and AMg4 alloys with scandium were obtained in the form of total equation:

$$C_p^0 = a + bT + cT^2 + dT^3. \quad (9)$$

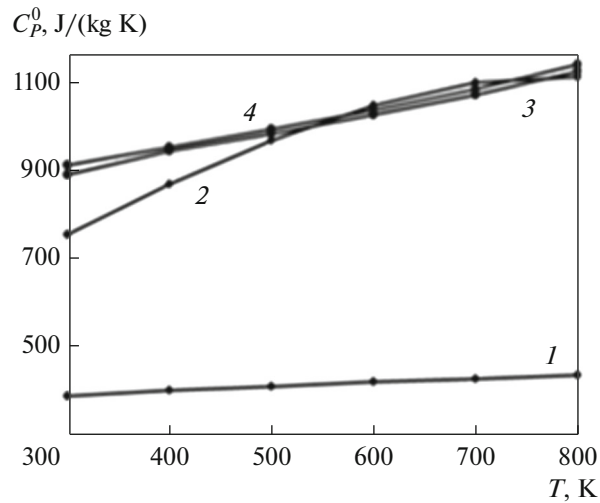


Fig. 6. Temperature dependences of the specific heat capacity of (1) copper and (2) AMg2, (3) AMg3, and (4) AMg4 alloys with 0.5 wt % scandium.

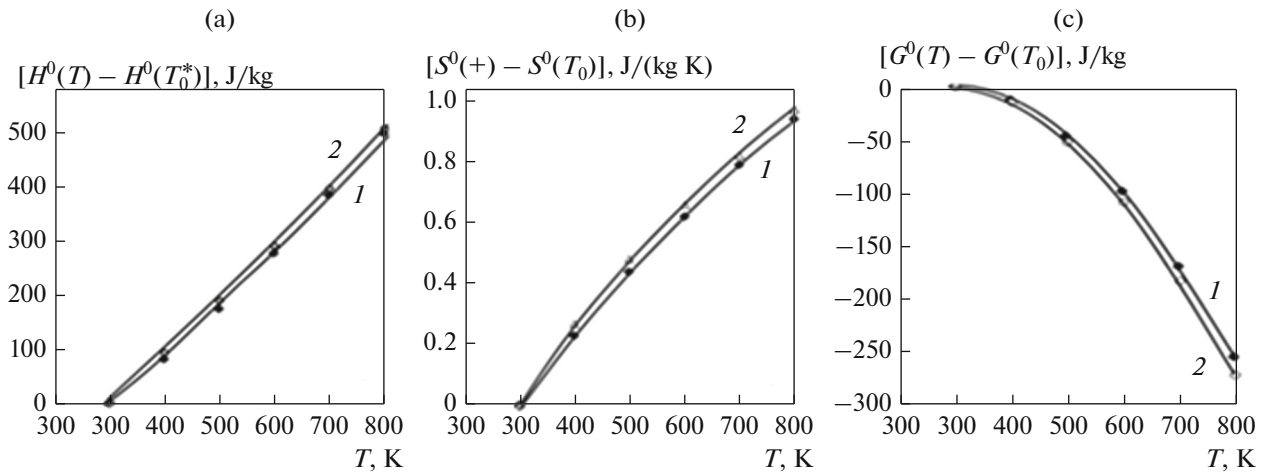


Fig. 7. Temperature dependences of changes in the specific (a) enthalpy, (b) entropy, and (c) Gibbs energy of the (1) AMg2 and (2) AMg4 alloys.

Figure 6 shows the heat capacity calculated (at a step of 100 K) by Eqs. (6) and (9). To calculate the temperature dependences of the specific enthalpy, entropy, and Gibbs energy changes by Eqs. (10)–(12), the heat capacity integrals determined by Eq. (9) were used:

$$\begin{aligned} [H^0(T) - H^0(T_0)] &= a(T - T_0) \\ &+ \frac{b}{2}(T^2 - T_0^2) + \frac{c}{3}(T^3 - T_0^3) + \frac{d}{4}(T^4 - T_0^4); \end{aligned} \quad (10)$$

$$\begin{aligned} [S^0(T) - S^0(T_0)] &= a \ln \frac{T}{T_0} + b(T - T_0) \\ &+ \frac{c}{2}(T^2 - T_0^2) + \frac{d}{3}(T^3 - T_0^3); \end{aligned} \quad (11)$$

$$\begin{aligned} [G^0(T) - G^0(T_0)] &= [H^0(T) - H^0(T_0)] \\ &- T[S^0(T) - S^0(T_0)], \end{aligned} \quad (12)$$

where $T_0 = 298.15$ K.

Figure 7 shows the temperature dependences of the enthalpy and entropy changes and Gibbs energy for the AMg2 and AMg4 alloys, which were calculated by Eqs. (10)–(12) at a step of 100 K.

CONCLUSIONS

(1) The specific heat capacity of the AMg2, AMg3, and AMg4 alloys with scandium was determined in the cooling regime. Mathematic models describing the temperature dependences of the heat capacity and

changes in thermodynamic functions (enthalpy, entropy, and Gibbs energy) of the alloys in a temperature range of 300–800 K were obtained.

(2) It is shown that, as the temperature increases, the specific heat capacity, enthalpy, and entropy of the alloys increase, whereas the value of the specific Gibbs energy decreases.

(3) It was found that scandium additions in a studied concentration range of 0.01–0.5 wt % almost do not affect the values of the specific heat capacity and changes in the thermodynamic functions of the initial AMg₂, AMg₃, and AMg₄ alloys.

REFERENCES

1. V. M. Beletskii and G. A. Krivov, *Aluminum Alloys (Composition, Properties, Technology, Application): A Handbook*, Ed. by I. N. Fridlyander (KOMITEKh, Kiev, 2005) [in Russian].
2. L. I. Kaigorodova, D. Yu. Rasposienko, V. G. Pushin, V. P. Pilyugin, and S. V. Smirnov, "Effect of Annealing on the structure and properties of the aging Al–Li–Cu–Mg–Zr–Sc–Zn alloy subjected to megaplastic strain," *Phys. Met. Metallogr.* **120**, 157–163 (2019).
3. S. Nazarov, S. Rossi, P. Bison, I. Ganiev, L. Pezzato, and I. Calliari, "Influence of rare earths addition on the properties of Al–Li alloys," *Phys. Met. Metallogr.* **120**, 402–409 (2019).
4. V. V. Krasnoyarskii and N. R. Saidaliev, "Corrosion-electrochemical properties of aluminum alloys with iron in neutral solutions," *Zashch. Korroz. Okruzh. Sredy*, No. **3**, 14–19 (1991).
5. V. F. Frolov, S. V. Belyaev, I. Yu. Gubanov, A. I. Bezrukikh, and I. V. Kostin, "The influence of technological factors on the formation of structure defects in large-tonnage ingots from aluminum alloys of the series 1XXX," *Vestn. MGTU im. G. I. Nosova* **14**, 25–31 (2016).
6. M. V. Chukin, V. M. Salganik, P. P. Poletskov, A. S. Kuznetsova, G. A. Berezhnaya, and M. S. Gushchina, "The main types and applications of nanostructured high-strength sheet metal," *Vestn. MGTU im. G.I. Nosova*, No. **4**, 41–44 (2014).
7. X. G. Chen, "Growth mechanisms of intermetallic phases in DC cast AA1XXX alloys," in *Essential Readings in Light Metals. V. 3. Cast Shop for Aluminum Production* (2013), pp. 460–465.
8. D. A. Grange, "Microstructure control in ingots of aluminum alloys with an emphasis on grain refinement," in *Essential Readings in Light Metals. V. 3. Cast Shop for Aluminum Production* (2013), pp. 354–365.
9. Geoffrey K. Sigworth, "Fundamentals of solidification in aluminum castings," *Int. J. Met. Casting* **8** (1), 7–20 (2014).
10. N. F. Ibrokhimov, I. N. Ganiev, Z. Nizomov, N. I. Ganieva, S. Zh. Ibrokhimov, "Effect of cerium on the thermophysical properties of AMg₂ alloy," *Phys. Met. Metallogr.* **117**, 49–53 (2016).
11. Kh. Kh. Azimov, I. N. Ganiev, I. T. Amonov, and N. F. Ibrokhimov, "The effect of lithium on the heat capacity and changes in the thermodynamic functions of the aluminum alloy AZh_{2.18}," *Vestn. MGTU im. G.I. Nosova* **16**, 37–44 (2018).
12. I. N. Ganiev, A. G. Safarov, F. R. Odinaev, U. Sh. Yakubov, and K. Kabutov, "Temperature dependence of the specific heat and changes in the thermodynamic functions of the alloy AZh_{4.5} with tin," *Izv. Vyssh. Uchebn. Zaved., Tsvetn. Metall.*, No. **1**, 50–58 (2019).
13. S. E. Otadzhonov, I. N. Ganiev, M. Makhmudov, and M. M. Sangov, "Temperature dependence of heat capacity and changes in the thermodynamic function of an AK1M2 alloy with calcium," *Izv. Yugo-Zapad. Gos. Un-ta. Ser. Tekh. Tekhnol.*, No. **3**(28), 105–115 (2018).
14. U. Sh. Yakubov, I. N. Ganiev, M. M. Makhmadizoda, A. G. Safarov, and N. I. Ganieva, "The effect of strontium on the temperature dependence of specific heat and changes in the thermodynamic functions of the alloy AZh_{5K10}," *Vestn. Sankt-Peterburg. Gos. Univ. Tekhnol. Dizain. Ser. Estestv. Nauk*, No. **3**, 61–67 (2018).
15. Dzh. Kh. Dzhailev, I. N. Ganiev, A. Kh. Khakimov, N. F. Ibrokhimov, and Kh. Kh. Azimov, "The effect of barium on the temperature dependence of specific heat and changes in the thermodynamic functions of the alloy AZh_{2.18}," *Vestn. TNU. Ser. Estestv. Nauk*, No. **4**, 240–248 (2018).
16. V. E. Zinov'ev, *Thermophysical Properties of Metals at High Temperatures* (Metallurgiya, Moscow, 1989) [in Russian].
17. *Thermodynamic Properties of Individual Substances. A Handbook*, Ed. by V. P. Glushkov (Nauka, Moscow, 1982) [in Russian].

Translated by N. Kolchugina